International Journal of Bio-Science and Bio-Technology
Vol.8, No.2 (2016), pp.45-62
http://dx.doi.org/10.14257/ijbsbt.2016.8.2.05

Synchronization of SA and AV Node Oscillators Using PSO Optimized RBF-based Controllers and Comparison with SMC

Abdolhossein Ayoubi[1]*, Moharram Kazemi [2], Mohammad Sadegh Sanie [3] and Saman Sobh Heydari[4]

[1,2,4]MSc of Medical Information Technology, Biomedical Engineering Department, Amirkabir University of Technology, Tehran, Iran
[3] MD in Anesthesia and critical care Department, Assistant Professor at Jahrom University of Medical Science, Iran
[1]ayoubi.hossein@gmail.com;[2]kazemi1az@yahoo.com, [3]Sadegh_532@yahoo.com, [4]saman303@yahoo.com

Abstract

This paper studies the synchronization of SA and AV Node Oscillators using PSO optimized RBF-based controllers systems. High levels of control activities may excite unmodeled dynamics of a system. This matter changes the rules of controlling the system and achieving an acceptable control performance. In fact, the objective here is to reach a trade-off between tracking performance and parametric uncertainty. Two methods are proposed to synchronize the general forms of Van Der Pol (VDP) Model and their performance. These methods use the radial basis function (RBF)- based neural controllers for this purpose. The first method uses a standard RBF neural controller. Particle swarm optimization (PSO) algorithm is used to derive and optimize the parameters of the RBF controller. In the second method, with the aim of increasing the robustness of the RBF controller, an error integral term is added to the equations of RBF neural network. For this method, the coefficients of the error integral component and the parameters of RBF neural network are also derived and optimized via PSO algorithm. For better comparison, simulation results show the effectiveness and superiority of the proposed methods in both performances in comparison with SMC controller.

Keywords*: Synchronization, Van der Pol Model, SA and AV Node Oscillators, SMC*

1. Introduction

The present paper examines synchronizations for Van der Pol oscillatory systems. Synchronization problem has found many applications in laser, chemical reactors, secure communications, and biology. This paper deals with one such application in cardiac synchronization. This is particularly important as cardiovascular diseases are among the major causes of death worldwide. Disruption in the electrical function of the heart is a type of such diseases generally referred to as "cardiac arrhythmia". Thus, electrical conduction system of the heart can be modeled and used in preventing serious heart diseases. One practical way to investigate how a member of an organism works is to develop a model which accurately reflects the function of this part. Such a model may serve as a hypothesis for some physiological observations. For simulating how stimulation propagates over the heart tissue, it seems necessary to develop an accurate model of cells action potential. For this purpose, Van der Pol model was used in the

[1] . **ayoubi.hossein@gmail.com, ayoubi@aut.ac.ir; Tel: +989171912965; Address: 7th Andisheh st, Moallem Ave, Jahrom, Fars, Iran, Postal code: 7417766486, Iran, P.O.Box: 445, Jahrom, Iran*

ISSN: 2233-7849 IJBSBT

present study to examine synchronization of heart oscillators. The main goal of this study is to synchronize atrio-ventricular (AV) oscillator with sino-atrial oscillator based on a particular model and by using different methods.

How pacemakers, including SA node and AV node, can be resynchronized in cases where one is out of synch with the other (this is a major cause of arrhythmia) will also be discussed.

2. An Overview of Cardiovascular Physiology

The heart will not be able to pump unless it receives an electrical excitation which originates from pumping. Generation and transmission of electrical impulses depend on automaticity, excitability, conductivity, and contractibility of cardiac cells. Transmission of cardiac impulses creates depolarization-repolarization cycles in cardiac cells. When at rest, the cardiac cells are polarized, *i.e*. they show no sign of electrical activity. The cell membranes separate different concentrations of such ions as K^+ and Na^+ and create larger negative charges inside the cell. The phenomenon is known as resting membrane potential. As soon as an electrical excitation arrives, the ions are transported at either side of the cell membrane leading to action potential or depolarization. Once a cell is completely depolarized, it tries to return to its initial conditions or resting state. This process is referred to as repolarization. The electrical charges are reversed and returned to the normal state. A typical depolarization-repolarization cycle consists of five phases (0 to 4) (Figure 1 presents action potential curve and variations in voltage in these five phases):

Phase 0: A cell receives an impulse from its adjacent cell and becomes depolarized.
Phase 1: An initial immediate repolarization takes place.
Phase 2: This slow repolarization step is also known as Plateau phase. In Phase 1, Phase 2, and early in Phase 3, cardiac cells are at total inexcitability state. In this phase, not every stimulus with any intensity can result in cellular response.
Phase 3: This phase is known as rapid repolarization. At this time, the cell returns to its initial state. At the last one-third of this phase, when the cell enters the relative excitability state, very strong excitations can depolarize it.
Phase 4: This step is the resting state for action potential. By the end of the fourth phase, the cell is ready for next excitations. All these activities can be recorded on electrocardiogram (ECG).

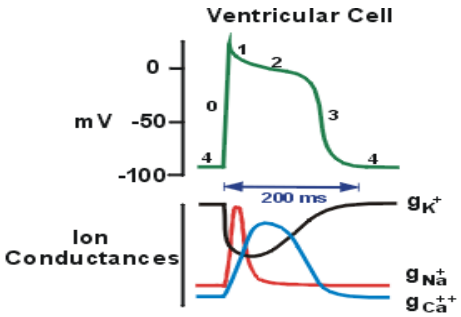

Figure 1. Action Potential Curve

2.1. Electromechanical Conduction Mechanism of the Heart

Immediately after depolarization and repolarization, electrical impulses propagate along a pathway known as conduction system (Figure 2). These impulses start traveling out of the SA node, through the atrium and Bachmann's bundle, and into the AV node. The impulses then travel through the bundle of His, left and right branches, and eventually into the Purkinje fibers. This conduction system is an electromechanical one. The electrical section orders the contraction of all cells, and the mechanical section

(cardiac muscles) implements these orders. Some diseases are caused by failure in these mechanical functions while most diseases are the result of the malfunction of electrical system. Heart electrical conduction system can be thought of as a self-exciting pacemaker. This system is responsible for proper and synchronized contraction of cardiac muscles [2].

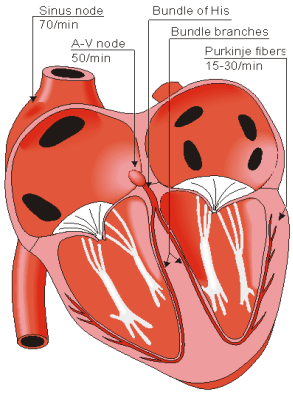

Figure 2. Pacemakers and Impulses Routes

3. Introduction to Synchronization

The word "synchronous" has its origin in the Greek word which means "sharing the same time period", and since its origin, the word has been used in everyday applications to denote agreement or dependency of the different processes in terms of time. Historically, synchronization analysis of dynamic systems has received considerable attention as a very important subject in physics. The phenomenon dates back to the 17th century when Hyugens patented two synchronized pendulum clocks with very weakly coupled oscillations.

In synchronization of oscillatory systems, two identical systems oscillate, simultaneously. If one system is designated as master and another identical system is assigned as slave when a proper control input is applied to the slave, the dynamic behavior or the two systems will become identical after a period of time. The slave which often have to become synchronized with the master is usually referred to as the response system or should be received while the master is sometimes called the drive or sender. The figure below, for example, shows synchronization of state trajectories of two systems after a few seconds.

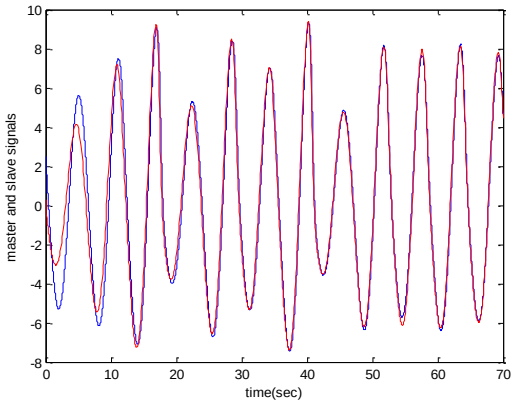

Figure 3. Synchronization

As mentioned earlier, the objective here is to synchronize the slave with the master. For this purpose, a nonlinear control system must be designed to receive the control signals from the master and to control the slave.

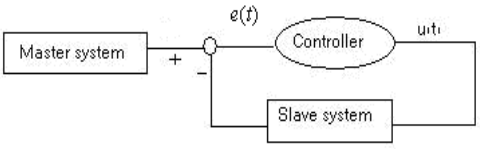

Figure 4. A Schematic of Master-slave Combination

Figure four presents a schematic of a master-slave system. Here, the slave behavior is clearly controlled by the master. In addition, the slave may have conditions different from those of the master.

3.1. Van Der Pol (VDP) Model

The first attempts to explain oscillatory behavior of the heart cells was made in 1926 by Van der Pol [34]. Balthasar van der Pol was a German physicist and an electronic engineer. He discovered stable oscillations, which are called limit cycle. Van der Pol was the first person to examine relaxation oscillations by studying an electrical circuit which had self-entertained oscillations with the amplitude independent of initial conditions. The schematic of this circuit is shown in Figure 5.

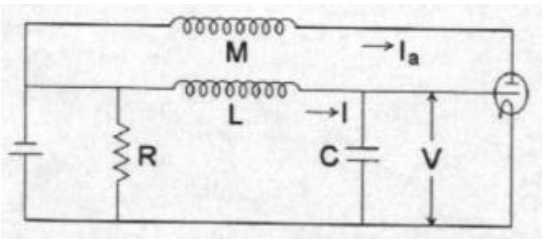

Figure 5. Van der Pol's Circuit

The equations of the voltages and currents in this circuit are

$$I_a = CV'(\theta) \quad I_a = V - \frac{1}{3}V^3, \quad , \quad L\frac{dI}{d\theta} + RI + V = M\frac{dI_a}{d\theta} \tag{1}$$

where

$$c = \frac{M}{\sqrt{LC}} - R\sqrt{\frac{C}{L}} \quad , \quad \theta = t\sqrt{LC} \quad V = x\sqrt{1 - R\frac{C}{M}} \tag{2}$$

By substitution *x*, *t*, and *c* from (2) into the current-voltage equations in (1), the following differential equation, known as Van der Pol's equation, is obtained:

$$\frac{d^2x}{dt^2} + c(x^2 - 1)\frac{dx}{dt} + x = 0$$

This circuit serves as an essential model for self-entertained oscillations in physics, electronic engineering, biology, neurology and many other sciences. Since *c* is the control parameter in this equation, different periodic responses can be initiated by changing the value of *c* with large values of *c* resulting in relaxation oscillations.

For some important properties, Van der Pol nonlinear equations are used to model the oscillations in the heart. First, Van der Pol oscillator adjusts its natural frequency to the input signal frequency without changing the oscillation amplitude. This is critically important as the low-frequency slave oscillator has to adjust itself to the dominant high-frequency pacemaker of the heart.

Therefore, Van der Pol model was used in this project to model the oscillators at SA and AV nodes. Each oscillator at SA node and AV node is modeled using Van der Pol differential equations. The interaction between the oscillators of the heart is modeled by the following Van der Pol equations. The coupling between these interacting oscillators is modeled as follows:

$$SA: \begin{cases} \dot{x}_1 = x_2 \\ \dot{x}_2 = -w_1^2 x_1 + c_1(\mu - x_1^2)x_2 + R_1(x_4 - x_2) \end{cases} \quad (3)$$

$$AV: \begin{cases} \dot{x}_3 = x_4 \\ \dot{x}_4 = -w_2^2 x_3 + c_2(\mu - x_3^2)x_4 + R_2(x_2 - x_4) + u \end{cases} \quad (4)$$

The first equation which models SA oscillations is the drive in the present synchronization problem while the second equation for modeling AV oscillations represents the response system.

4. Generating Action Potential by the Model

Heart rhythm is determined by a series of electric impulses (action potential) which travel throughout the heart. The figures below show action potentials for SA and AV cells obtained through.

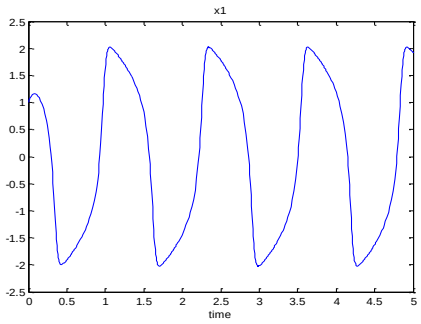

Figure 6. Simulating Van der Pol Model in MATLAB

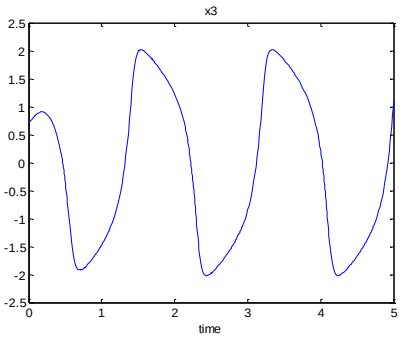

Figure 7. Action Potential Waveforms

These figures demonstrate the validity of the Van der Pol model used here in terms of how these waveforms match the actual forms generated in the heart.

5. Designing Sliding Mode Controller

Sliding mode control provides a robust controller for nonlinear dynamic systems although it involves a discrete-time control factor which may lead to chattering in a neighborhood of the sliding surface. One common solution to reduce chattering is to introduce a boundary layer in the vicinity of the sliding surface [11]. This can improve closed-loop stability and resolve chattering, but a finite steady-state error will exist as a result of finite steady-state error gain in the control algorithm.

The proposed controller provides a desirable transient state as well as a robust performance. In addition, it combines PI control and SMC to prevent chattering. It will be demonstrated that the closed-loop system is globally stable in the sense of Lyapunov (I.S.L.), and that the output of the system can asymptotically track the reference input by modeling uncertainties and disturbances.

6. Problem Definition

A typical nonlinear SISO system of order *n* can be shown as

$$x^{(n)} = f(\underline{x}, t) + g(\underline{x}, t)u + a(t)$$
$$y = x \tag{5}$$

where f and g are unknown nonlinear functions, and $\underline{x} = [x, \dot{x}, \ldots, x^{(n-1)}]^T = [x_1, x_2, \ldots, x_n]^T \in R^n$ is the state vector of the system, assumed to be measurable. $u \in R$ and $y \in R$ represent the system input and output, respectively and *d(t)* is an unknown outer disturbance. It is assumed that *d(t)* is bounded by the upper bound *D*; *i.e. d(t)* $\leq D$. For the system (5) to be controllable, we must have $g(\underline{x}, t) \neq 0$. Therefore, we assume that $g(\underline{x}, t) > 0$. The control problem is to find the state *x* for tracking the desirable state x_d in the presence of uncertainties and outer disturbances with the following tracking error:

$$\underline{e} = \underline{x} - \underline{x}_d \left[e, \dot{e}, \ldots, e^{(n-1)}\right]^T \in R^n \tag{6}$$

The sliding surface for the state error can be determined as

$$s(e) = c_1 e + c_2 \dot{e} + \cdots + c_{n-1} e^{(n-2)} + e^{(n-1)} = \underline{c}^T \underline{e} \tag{7}$$

where $\underline{c} = [c_1, c_2, \ldots, c_{n-1}, 1]^T$ represents the coefficients of the Hurwitz polynomial $h(\lambda) = \lambda^{n-1} + c_{n-1}\lambda^{n-2} + \cdots + c_1$. All roots lie in the left-hand plane; and λ is the Laplace operator. If the initial condition *e(0)=0* holds, in the tracking problem $\underline{x} = \underline{x}_d$, an error vector on the state space may be defined on the sliding surface *s(e)=0* for all *t>0*. A sufficient condition for this is to choose a control strategy as

$$\frac{1}{2}\frac{d}{dt}s^2(\underline{e}) \leq -\eta|s| \quad , \quad \eta \geq 0 \tag{8}$$

The state of the controlled system always moves toward the sliding surface. The sign of the control signal must switch based on the state trajectory and the sliding surface. Consider the nonlinear control problem shown in (5). If $f(\underline{x}, t)$ and $g(\underline{x}, t)$ are known, the SMC input *u** satisfies the sliding condition (8).

$$u^* = \frac{1}{g(\underline{x}, t)}\left[-\sum_{i=1}^{n-1} c_i e^{(i)} - f(\underline{x}, t) + x_d^{(n)} - \eta sng(s)\right] \tag{9}$$

where

$$sng(s) = \begin{cases} 1 & for \quad s > 0 \\ 0 & for \quad s = 0 \\ -1 & for \quad s < 0 \end{cases} \tag{10}$$

A Lyapunov candidate function is defined as:

$$V_1 = \frac{1}{2}\mathrm{s}^2(\underline{\mathrm{e}}) \tag{11}$$

By differentiating (11) with respect to time, $\dot{V}$ for the system trajectory is obtained:

$$\dot{V} = s.\dot{s} = s.\left(c_1\dot{e} + c_2\ddot{e} + \cdots + c_{n-1}e^{(n-1)} + x^{(n)} + x_d^{(n)}\right) \tag{12}$$

$$= s.\left(\sum_{i=1}^{n-1} c_i e^{(i)} + f(\underline{x},t) + g(\underline{x},t)u + d(t) - x_d^{(n)}\right) \leq -\eta|s|$$

Therefore, the SMC input u^* satisfies the sliding condition (8). Clearly, to satisfy this condition, an impulsive control condition must be added in the form of $u^* = u_{eq} - u_{sw}$ where

$$u_{eq} = g(\underline{x},t)^{-1}\left[-\sum_{i=1}^{n-1} c_i e^{(i)} - f(\underline{x},t) + x_d^{(n)}\right] \tag{13}$$

$$u_{sw} = -g(\underline{x},t)^{-1}.\eta sng(s) \tag{14}$$

But since *f* and *g* are still unknown, it is difficult to apply the control law (9) to an unknown nonlinear system. Moreover, the switching type condition u_{sw} will create chattering.

7. Synchronization Using SMC

Using the SMC technique, the problem of the controller design is divided into two independent steps:
Step 1: Selecting a sliding surface for desirable sliding movement
Step 2: Designing a controller to move any trajectory within the state space toward the sliding surface, where a non-continuous controller can be used to maintain the ultimate state on this surface. A special characteristic of this control mechanism is that while it is in the sliding mode, the system is robust with respect to parameter uncertainty and outer disturbances.
For this purpose, first a sliding surface must be selected; *i.e.* a time-varying surface *s(t)* is defined as

$$s = \sum_{j=1}^{\rho-1} k_j e_j + e_\rho \tag{15}$$

where e_j is the state error and ρ is relative degree, and the positive constants *k* are chosen so that the following polynomial becomes a Hurwitz polynomial:

$$\lambda^{\rho-1} + k_{\rho-1}\lambda^{\rho-2} + \ldots + k_1 \tag{16}$$

This condition ensures that the movements will be limited to the surface *s=0* and, therefore, the tracking errors $e=x-x_d$ (where x_d represents the desirable states) will converge to zero. Sliding mode or sliding state refers to the behavior of the system on the sliding surface.

A feedback control law *u* is selected in a way that satisfies the sliding condition. However, in order to account for uncertainties in modeling and disturbances, the control

law must be non-continuous on *s(t)*. Since the switching control law may not be implemented perfectly (for example, the switching does not occur instantly, and *s* is not known with infinite accuracy), this results in chattering which is not desirable in practical applications because it increases control activities and may also excite high-frequency dynamics (*e.g.* unmodeled structural modes, neglected delays, *etc*) which have not been considered during modeling.
It is shown the sliding mode dynamics as $\dot{s} = 0$.

By solving the equation above, an expression, known as equivalent control u_{eq}, is found for *u*. It can be thought of as a continuous control law which satisfies $\dot{s} = 0$ if the dynamics are known.

As noted in the previous sections, the equations for SA and AV are in the following forms:

$$\begin{aligned} SA &: \ \ddot{x}_d = -x_d + c_1(1 - x_d^2)\dot{x}_d \\ AV &: \ \ddot{x} = -x + c_2(1 - x^2)\dot{x} + R(\dot{x}_d - \dot{x}) + u \end{aligned} \tag{17}$$

where c_2 is assumed to contain uncertainty.

The objective in the synchronization problem is to make AV oscillator tracj SA oscillator. Therefore, for the system above to track $x(t) \equiv x_d(t)$, sliding surface is defined as

$$\begin{aligned} S &= (\frac{d}{dt} + \lambda)^{(\rho-1)}\tilde{x} = \tilde{\tilde{x}} + \lambda\tilde{x} \\ \tilde{x} &= x - x_d \end{aligned} \tag{18}$$

where *s(t)* is both a dynamic and a locus.

$$\begin{aligned} \dot{S} &= \dot{\tilde{\tilde{x}}} + \lambda\dot{\tilde{x}} = \ddot{x} - \ddot{x}_d + \lambda\dot{\tilde{x}} \\ &= -x + c_2(1 - x^2)\dot{x} + R\dot{\tilde{x}}_d + u - \ddot{x}_d + \lambda\dot{\tilde{x}} = 0 \end{aligned} \tag{19}$$

Then:

$$u_{eq} = x - c_2(1 - x^2)\dot{x} - R\dot{x}_d + \ddot{x}_d - \lambda\dot{\tilde{x}} \tag{20}$$

Thus, equivalent control is obtained. The above value for *u* cannot be calculated since c_2 is unknown. Suppose that $\hat{c}_2 = c_2 + \Delta c_2$, where Δc_2 represents parameter uncertainty. Hence, for *u*:

$$\begin{aligned} \hat{u}_{eq} &= x - \hat{c}_2(1 - x^2)\dot{x} - R\dot{\tilde{x}}_d + \ddot{x}_d - \lambda\dot{\tilde{x}} \\ \Rightarrow \dot{S} &= (c_2 - \hat{c}_2)(1 - x^2)\dot{x} \neq 0 \end{aligned} \tag{21}$$

In order to hold the sliding condition, despite the uncertainties in the system dynamics, a discontinuous term is added to $\hat{u}_{eq}$ on the surface *s=0*:

$$\begin{aligned} u &= \hat{u}_{eq} - k\,\mathrm{sgn}(S) \\ \Rightarrow \dot{S} &= (c_2 - \hat{c}_2)(1 - x^2)\dot{x} - k\,\mathrm{sgn}(S) \end{aligned} \tag{22}$$

where *sgn* is the sign function, and *k* is defined as follows in a way that the sliding conditions are met and sliding mode movement occurs.

$$k = (c_2 - \hat{c}_2)(1 - x^2)\dot{x} + \eta, \qquad \eta > 0 \tag{23}$$

As seen here, discontinuity of *k* on the surface *s=0* increases with the parameter uncertainty. By choosing a proper value for *k*, it is possible to reduce chattering as well as the time needed for attaining sliding mode [51]. This ensures that *s* will converge to zero within a finite time and will remain at this value for all subsequent times, and therefore, the errors e_1 and e_2 will asymptotically approach zero. However, this technique my lead to excitation of unmodeled high-frequency dynamics or improper switching within the system, thereby deteriorating the system performance or even causing instability. Researchers, therefore, always tried to address this issue. For this purpose, different methods have been employed to reduce or eliminate this type of excitation. One common technique used to resolve this problem is to replace discontinuous control with a continuous approximation. In this way, the discontinuous function *sgn(s)* is replaced with its continuous approximation *sat(s)*. This technique works well in resolving the problem but often at the expense of a non-zero steady-state error. Here, an appropriate method for synchronizing two oscillators with parameter uncertainty and even with different structures is proposed.

7.1. Stability

To observe dynamic stability of error in the proposed controller, the Lyapunov candidate function $V=s^2/2$ was chosen. The derivative of *V* is given by

$$\dot{v} = \dot{S}S = [(c_2 - \hat{c}_2)(1 - x^2)\dot{x} - k\,\mathrm{sgn}(S)]S$$
$$\Rightarrow \dot{v} = [(c_2 - \hat{c}_2)(1 - x^2)\dot{x} - \left|(c_2 - \hat{c}_2)(1 - x^2)\dot{x}\right|]\left|S\right| - \eta\left|S\right| < 0 \tag{24}$$

Note that *sgn(s)* is always positive as long as *k>0* and *e≠0*.

Since *V* is a positive and decrescent function and $\dot{V}$ is negative definite, the equilibrium point $(e_i = 0, i = 1, \ldots, n)$ is uniformly stable; that is, $e_i(t) \in L_\infty$. It can be easily shown that $e_i(t), i = 1, \ldots, n$ are square-integrable with respect to *t*; *i.e.* $e_i \in L_2$. According to Barbalat's Lemma, and for any initial conditions, we have $\dot{e}_i(t) \in L_\infty$,which means $e_i(t) \to 0$ as $t \to \infty$. Thus, S asymptotically converges to zero. Therefore, $x \to x_d$ when $t \to \infty$. This shows that the SMC has synchronized the two systems.

7.2. Simulation Results

To demonstrate the capabilities of the proposed method, in this section synchronization is carried out for two sample systems. The descriptive equations for the SA and AV oscillators are:

$$SA: \begin{cases} \dot{x}_1 = x_2 \\ \dot{x}_2 = -w_1^{\,2} x_1 + c_1(1 - x_1^2)x_2 \end{cases}$$
$$AV: \begin{cases} \dot{x}_3 = x_4 \\ \dot{x}_4 = -w_2^{\,2} x_3 + c_2(1 - x_3^2)x_4 + R(x_2 - x_4) + u \end{cases} \tag{25}$$

The initial conditions for the master and slave are (1,4) and (0.7, 2), respectively. Based on the physiological facts, a one-way coupling is considered here. The frequency is 60 pulses per minute for the first oscillator and 40 pulses per minute for the second oscillator. It is assumed that c2 contains uncertainty and $\hat{c}_2 = c_2 + \Delta c_2$ where Δc_2 represents uncertainty. SA and AV oscillators, synchronized by the proposed method despite parameter uncertainty, are shown in Figure 8.

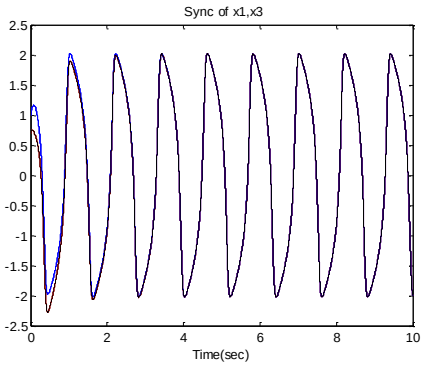

Figure 8. Synchronization Using SMC

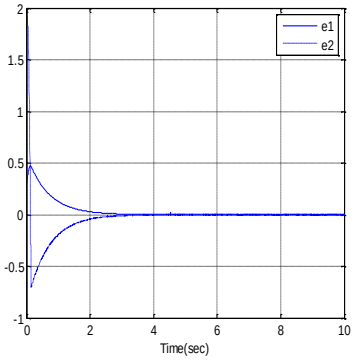

Figure 9. Synchronization Error: Diminished Over Time

8. PSO Algorithm

PSO is a population-based stochastic optimization technique which does not use the gradient of the problem being optimized, so it does not require being differentiable for the optimization problem as is necessary in classic optimization algorithms. Therefore, it can also be used in optimization problems that are partially irregular, time variable and noisy. In PSO algorithm, each bird, referred to as a "particle", represents a possible solution for the problem. Each particle moves through the D-dimensional problem space by updating its velocities with the best solution found by itself (cognitive behavior) and the best solution found by any particle in its neighborhood (social behavior). Particles move in a multidimensional search space, and each particle has a velocity and a position as follows:

$$v_i(k+1) = v_i(k) + \gamma_{1i}\left(P_i - x_i(k)\right) + \gamma_{2i}\left(G - x_i(k)\right) \quad (26)$$

$$x_i(k+1) = x_i(k) + v_i(k+1) \quad (27)$$

where i is the particle index; k is the discrete-time index; vi is the velocity of ith particle; xi is the position of ith particle; Pi is the best position found by i^{th} particle (personal best); G is the best position found by swarm (global best), and γ1,2 are random numbers in the interval [0, 1] applied to ith particle. In our simulations, the following equation is used for velocity:

$$v_i(k+1) = \phi(k)v_i(k) + \beta_1[\gamma_{1i}\left(P_i - x_i(k)\right)] + \beta_2[\gamma_{2i}\left(G_i - x_i(k)\right)] \quad (28)$$

in which ϕ is inertia function and β1, β2 are acceleration constants. The flowchart of the standard PSO algorithm is depicted in Figure 10.

9. Proposed Synchronization Schemes

As mentioned before, the synchronization scheme consists of two systems: the master and the slave (Figure 11). In this scheme, an RBF- or "RBF + error integral"-based controller is used to make the states of the slave system follow the states of the master system, in the presence of uncertainties and external disturbances. It should be noted that in Figure 11 h(·) can be any continuous function. In this section, two proposed methods of systems synchronization are described: (14) RBF-based nonlinear controller, (15) "RBF + error integral" model in which an integral term is added to RBF model to improve the robustness of the proposed controller. To optimize the parameters of these controllers, PSO as a continuous evolutionary algorithm is also used. The mathematical formulation:

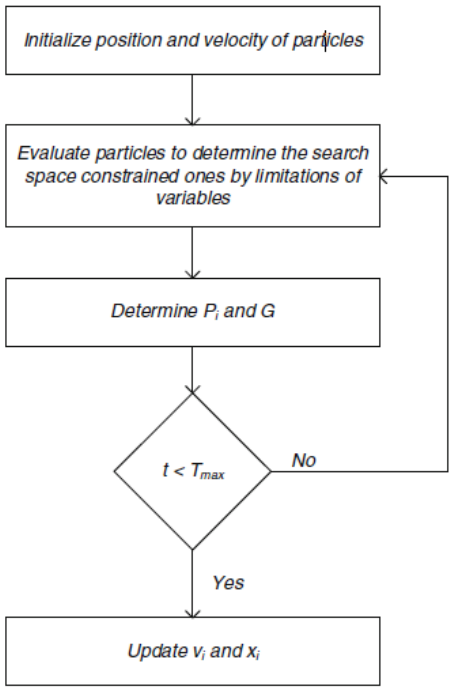

Figure 10. Flowchart of PSO Algorithm

Proposed methods are stated in the following subsections:

10. Control by RBF Model

Consider the control system in (15), for this system the following RBF-based controller is proposed:

$$u(t) = W^{T} \xi(e) \tag{29}$$

in which u(t) is the control signal, and $e = [e_1, e_2, ..., e_n]^T, e_i = x_{im} - x_{is}, i = 1,2,..., n, x_{im}$ and $x_{is}, i = 1,2,... n$ are the states of master and slave systems, respectively. $W = [w_1, w_2, ..., w_M]^T \in \Re^M$ is the weight matrix, and $\xi(e) = [\xi_1(e), \xi_2(e), ..., \xi_M(e)]^T \in \Re^M$ is a set of basis functions of the corresponding RBF model. The basis function $\xi_i(e)^M$ of ith node in the hidden layer is considered as a Gaussian function as:

$$\xi_i(e) = \exp\left(-\frac{\|e - c_i\|^2}{\delta_i^2}\right) \quad (30)$$

in which ci and δi are the center and the width, respectively. Considering $c = [c_1, c_2, ..., c_n]^T \in \Re^n$ and $\delta = [\delta_1, \delta_2, ..., \delta_n]^T \in R^n$ the goal is to find the optimized $W = W^*, c = c^*$ and $\delta = \delta^*$ such that the following cost functional is minimized:

$$IAE = \int_0^T \|e(t)\| dt \quad (31)$$

Where $\|.\|$ is the Euclidean norm of a vector. To find the optimized parameters $W = W^*, c = c^*$ and $\delta = \delta^*$, the PSO algorithm is used.

11. "RBF + Error Integral" Model

As mentioned before, there may be modeling uncertainties and external disturbances in the control problem. Therefore, the controller should be robust enough such that it can cope with these uncertainties. Now, as a modification of the method proposed, the integral components are added to the basis function vector to increase the robustness of the system. Therefore, the following controller is proposed:

$$u(t) = W_I^T \xi_1(e) \quad (32)$$

Where

$$W_I = [w_1, w_2, ..., w_M, w_{M+1}, w_{m+2}, ..., w_{M+n}]^T \in \Re^{M+n}, \xi_I(e) = [\xi_{1I}(e), \xi_{2I}(e), ..., \xi_{MI}(e), \int edt]^T \in \Re^{+n} \quad (33)$$

$\xi_{iI}(e) = \xi_i(e), i = 1,2,..., M$ and $\int edt = [\int e_1 dt, \int e_2 dt, ..., \int e_n dt] \in \Re$ .The goal in this scheme is to find the optimized $W = W^*, c = c^*$ and $\delta = \delta^*$ such that the cost functional (31) is minimized.

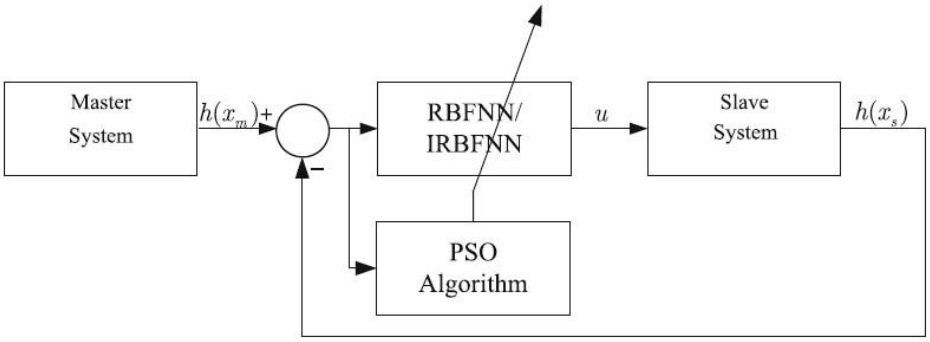

Figure 11. Block Diagram of Synchronization Scheme

12. Simulation and Experimental Results

Figure 3 illustrates the block diagram of system. As mentioned before, the system consists of a master and a slave. Considering $h(.)$ to be any continuous function, in system masking scheme, the message signal *m(t)* is added to the output of the master system, $h(x_m)$. The controller is designed such that the master and the slave systems are synchronized. Thus by subtracting the output of the slave system, $h(x_s)$, from the resulted signal, the message signal can be thoroughly recovered. It should be noted that the

controller should be designed such that it can cope with uncertainties and external disturbances.

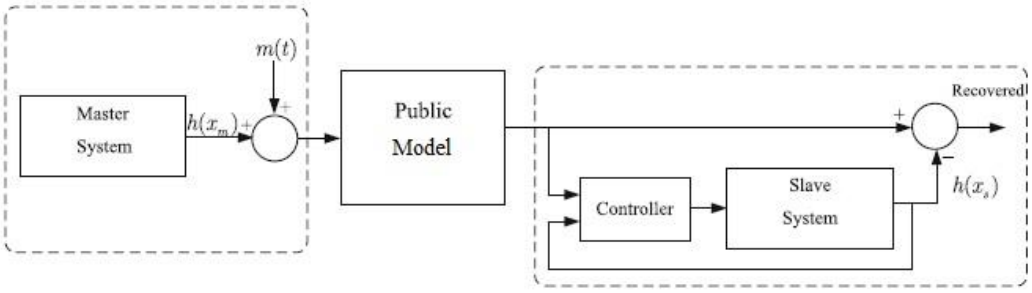

Figure 12. Block Diagram of System Masking Scheme

The descriptive equations for the SA and AV oscillators are:

$$SA: \begin{cases} \dot{x}_1 = x_2 \\ \dot{x}_2 = -w_1^{\,2} x_1 + c_1(1 - x_1^2)x_2 \end{cases}$$

$$AV: \begin{cases} \dot{x}_3 = x_4 \\ \dot{x}_4 = -w_2^{\,2} x_3 + c_2(1 - x_3^2)x_4 + R(x_2 - x_4) + u \end{cases}$$

The initial conditions for the master and slave are (1,4) and (0.7, 2), respectively. Based on the physiological facts, a one-way coupling is considered here. The frequency is 60 pulses per minute for the first oscillator, and 40 pulses per minute for the second oscillator. It is assumed that c2 contains uncertainty and $\hat{c}_2 = c_2 + \Delta c_2$ where Δc_2 represents uncertainty.

SA and AV oscillators, synchronized by the proposed method despite parameter uncertainty, are shown in Figure 14.

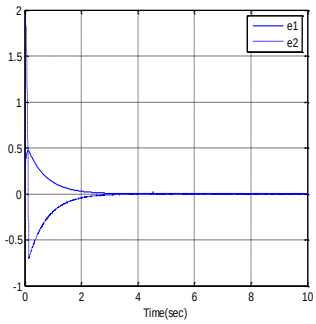

Figure 13. Synchronization Error: Diminished Over Time

Eventually, as seen in Figure (14), the system output converges to the desirable output.

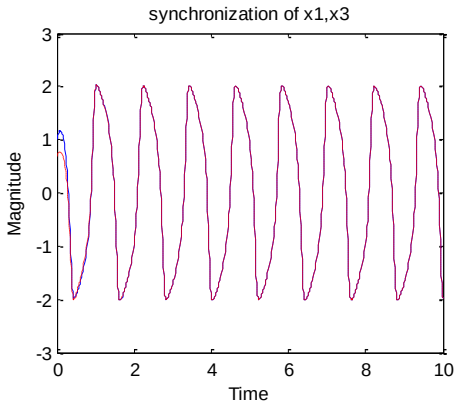

Figure 14. Synchronization Using PSO Optimized RBF-based Controllers

As seen in this figure, the SA and AV oscillators have become synchronized once a time period is passed.

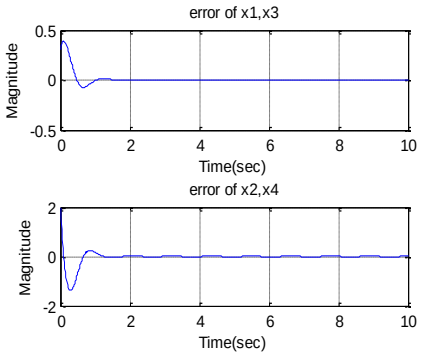

Figure 15. Synchronization Error

The figure above presents the synchronization error. This error vanishes over time indicating that the two oscillators have become synchronized.

13. Two-way Coupling

If two-way coupling is used for the two oscillators - which in physiological sense means that AV oscillator impacts SA oscillator as well, sometimes in a relatively weak manner – the equations become:

$$SA: \begin{cases} \dot{x}_1 = x_2 \\ \dot{x}_2 = -w_1^{\,2} x_1 + c_1(1 - x_1^2)x_2 + R_1(x_4 - x_2) \end{cases}$$

$$AV: \begin{cases} \dot{x}_3 = x_4 \\ \dot{x}_4 = -w_2^{\,2} x_3 + c_2(1 - x_3^2)x_4 + R_2(x_2 - x_4) + u \end{cases}$$

First, a value for R_1 which was about the one tenth of R_2 is selected. The computation results indicated that two-way coupling has no effect on synchronization time. The value of R_1 was then increased, but no impact was observed on synchronization time. This is in line with physiology of heart as AV oscillator has negligible effect on SA oscillator.

14. Conclusions

This paper examined the synchronization of SA and AV Node Oscillators using PSO optimized RBF-based controllers systems. It was observed that high levels of control

activities excited unmodeled dynamics of a system. Thus, changes in the rules of controlling the system occurred and an acceptable control performance was achieved. A trade-off between tracking performance and parametric uncertainty was also obtained. A standard RBF neural controller and particle swarm optimization (PSO) algorithm resulted in optimization of the parameters of the RBF controller. Robustness of the RBF controller was increased. The parameters of RBF neural network were also derived, and were optimized via PSO algorithm. Simulation results show the effectiveness and superiority of the proposed methods in both performances in comparison with SMC controller.

The table below shows the results of the two methods. As seen on the table, PSO optimized RBF-based controllers outperforms in terms of synchronization time and variance of error.

Table 1. Results of Two Methods: PSO Optimized RBF-based controllers outperforms

SA and AV Node Oscillators	Synchronization Time(sec)	Error Variance	Control Effort(max)	Control Effort (min)
PSO optimized RBF-based Controllers	0.2	0.001152	+149	-149
SMC Control	3.7	0.0032	+7.2	-31

Conflict of Interest

No conflict of interest.

References

[1] K. Grudzinski and J. Zebrowski, 'Modeling Cardiac Pacemakers With Relaxation Oscillators', Journal of Physica A: Statistical and Theoretical Physics, vol. 336, no.1, **(2004)**, pp. 153-162.

[2] E. P. Tsagalou, M. I. Anastasiou-Nana, L. A. Karagounis, G. P. Alexopoulos, C. Batziou, S. Toumanidis, E. Papadaki, J. N. Nanas and S. F. Stamatelopoulos, "Dispersion of QT and QRS in Patients with Severe Congestive Heart Failure: Relation to Cardiac and Sudden Death Mortality", The Hellenic Journal of Cardiology, (2002), vol. 43, pp. 209-215.

[3] S. A. Sivan and S. Akselrod, "A Phase Response Curve Based Model: Effect of Vagal and Sympathetic Stimulation and Interaction on Pacemaker cell, Journal of Theoretical Biology", (1998), vol. 192, no.4, pp. 567-579.

[4] K. Vibe, J. M. Vesin and E. Pruvot, "Chaos and Heart Rate Variability", International Conference of IEEE-EMBS and CMBEC, Physiological Systems/Modeling and Identification, (1997), pp.1481-1482.

[5] G. L. Gebber, S. Zhong, and S. M. Barman, "Synchronization of Cardiac-Related Discharges of Sympathetic Nerves With Inputs from Widely Separated Spinal Segments, American Journal of Physiology", (1995), vol. 268, no.6, pp. 1472-1483.

[6] G. L. Gebber, S. Zhong, S. M. Barman, and H. S. Orer, "Coordination of Cardiac-Related Discharges of sympathetic Nerves with Different Targets", American Journal of Physiology, (1994), vol. 167, no.2, pp. 400-407.

[7] S. Demir, J. Clark and W. Giles, "Effects of Hyperpolarizing Pulses on a Cardiac Pacemaker Cell", IEEE Transaction on Computer in Cardiology, (1997), vol. 24, pp. 713-716.

[8] J. Sundes, G. Lines and A. Tveito, "Efficient Solution of Ordinary Differential Equation Modeling Electrical Activity in Cardiac Cells", Mathematical Biosciences, (2002), vol. 72, pp. 55-72.

[9] C. H. Luo and Y. Rudy, "A Model of the Ventricular Cardiac Action Potential. Depolarization, repolarization, and their interaction", Circulation Research, (1991), vol. 68, no. 6, pp.1501-1562.

[10] T. H. Ma¨kikallio, MD, Heikki V. Huikuri, MD, FACC, Anne Ma¨kikallio, MD,Leif B. Sourander, MD, Raul D. Mitrani, MD, FACC, Agustin Castellanos, MD, FACC,Robert J. Myerburg, MD, FACC, 'Prediction of Sudden Cardiac Death by Fractal Analysis of Heart Rate Variability in Elderly Subjects', Journal of the American College of Cardiology , (2001), vol. 37, no. 5.

[11] K. Schafer, M. G. Rosenblum, J. Kurths and H. H. Abel, "Heartbeat Synchronized with Ventilation", Nature, vol. 392, (1998), pp. 239-240.

[12] Bernardo D. D., 'A Model of two Nonlinear Coupled Oscillators for the Study of Heart Beat Dynamics', International Journal of Bifurcation and Chaos, (1998); Vol. 8, No. 10, pp. 1975-1985.

[13] Dragoi V., and Grosu I., 'Synchronization of Locally Coupled Neural Oscillators', Neural Processing Letters, vol. 7, no.3, (1998), pp. 199-210.

[14] Volkov E. I., 'Limit Cycles Arising in a Chain Of Inhibitory Coupled Identical Relaxation Oscillators Near the Self-Oscillation Threshold', Radiophysics and Quantum Electronics, vol. 48, no. 3, (2005), pp. 212-221.
[15] E. Verheijck, R. Wilders, R. Joyner, D. Golod, R. Kumar, H. Jomgsma, L. Bouman and A. Ginneken, "Pacemaker Synchronization of Electrically Coupled Rabbit Sinoatrial Node Cell", Journal of General physiology, vol. 111, no.1, (1998), pp. 95-112.
[16] Y. Yu and S. Zhang, 'The Synchronization of Linearly Bidirectional Coupled Chaotic Systems', Chaos, Solitons and Fractals, vol. 22, no. 1, (2004), pp. 189–197.
[17] Y. Zhang and J. Sun, "Some Simple Global Synchronization Criterions for Coupled Time-Varying Chaotic Systems", Chaos, Solitons and Fractal, vol. 19, no.1, (2004), pp. 93–98.
[18] N. Buric, and D. Todorovic, "Dynamic of Fitzhugh-Nagumo Excitable Systems with Delayed Coupling", Physical review. E, Statistical, Nonlinear, and Soft Matter Physics, (2003), vol. 67, no.2, pp. 066222-1-066222-13 .
[19] G. L. Gebber, S. Zhong, S. Y. Zhou, and S. M. Barman, "Nonlinear dynamics of the frequency locking of baroreceptor and sympathetic rhythms", American Journal of Physiology., vol. 273, no.6, (1997), pp. 1932-1945 .
[20] V. d. pol & V. d. mark, "The Heartbeat Considered as a Relaxation Oscillation and an Electrical Model of the Heart", Philosophical Magazine 6, (1928); pp 763-775.
[21] Humg J.Y., Gao W.and Hung J.C., 'Variable structure control: A survey', IEEE Trans. Industrial Electron., (1993); vol. 40,pp. 2-22.
[22] Sato S., Doi S., and Nomura T., 'Bonhoeffer-van der Pol Oscillator Model of the SinoAtrial Node: A Possible Mechanism of Heart Rate Regulation', Method of Information in Medicine, March (1994);Vol. 33, No. 1, pp. 116-119.
[23] El-sherif N., Denes P., Katz R., Capone R., Brent L., Carlson M., Reynolds R., 'Definition of the Best Prediction Criteria of the Time Domain Signal-Averaged Electrocardiogram for Serious Arrhythmic Events in the Postinfarction Period', Journal of American College of Cardiology , March (1995);Vol. 25, No. 4, pp. 908-14.
[24] Kaplan B.Z., Gabay I., Sarafian G.and Sarafian D. 'Biological application of filtered van der pol oscillator', Journal of the Franklin Institute, (2007).
[25] Hao, Zh., Xi-Kui M.and Wei-Zeng L., 'Synchronization of Chaotic Systems with Parametric Uncertainty Using Active Sliding Mode Control', Chaos, Solutions and Fractals , September (2004),Vol. 21, No.5 , pp. 1249–1257.
[26] Thong T., McNames J., Aboy M. and Goldstein B., 'Prediction of Paroxysmal Atrial Fibrillation by Analysis of Atrial Premature Complexes', IEEE Transaction on biomedical Engineering, April (2004);Vol. 51, No. 4, pp. 561-569.
[27] Govindan R. B., Narayanan K., and Gopinathan M. S., 'On the Evidence of Deterministic Chaos in ECG: Surrogate and Predictability Analysis', Journal of Chaos , June (1998);Vol. 8, No. 2, pp. 495-502.
[28] Jungi L., and Parlitz U., 'Synchronization Using Dynamic Coupling, Physical review'. E, Statistical, Nonlinear, and Soft Matter Physics, November (2001);Vol. 64, No.2, pp.055204-1-055204-4.
[29] Hoyer D., Hoyer O.and Zwiener U., 'A New Approach to Uncover Dynamic Phase Coordination and Synchronization', IEEE Transaction on Biomedical Engineering, January (2000);Vol.47, No. 1, pp. 68-73.
[30] Thong T., McNames J., Aboy M. and Goldstein B., 'Paroxysmal Atrial Fibrillation Prediction Using Isolated Premature Atrial Events and Paroxysmal Atrial Tachycardia', proceedings of Annual International Conference of the IEEE Engineering in Medicine and Biology, September (2003);pp. 163-166.
[31] Jitao S., 'Global Synchronization Criteria with Channel Time-delay for Chaotic Time-delay System', Chaos, Solitons and Fractals, August (2004);Vol. 21, No.1, pp. 967–975.
[32] http://D. Noble; noble.physiol.ox.ac.uk/people/Dnoble
[33] Thong T. and Goldstein B., 'Prediction of Tachyarrhythmia Episodes', Joint Meeting of the IEEE EMBS and the BMES, October (2002);Houston, Texas.
[34] Slotine J.J.E. and Li W., 'Applied Nonlinear Control'. Prentice-Hall International Editions, Prentice-Hall International Edition,(1991).
[35] Wang Y., Guan Z.H. and Wen X.. 'Adaptive Synchronization for Chen Chaotic System with Fully Unknown Parameters', Chaos Solution and Fractals, March (2004);Vol. 19, No.4, pp. 899-903.
[36] C.Y. Su and Y. 'Stepanenko, of a Class of Nonlinear Systems with Fuzzy Logic', IEEE Trans. Fuzzy Syst., (1994),vol.2, pp.285-294.
[37] Sivan S. A. and Akselrod S., 'Simulation of Atrial Activity by a Phase Response Curve Based Model of Two-dimensional Pacemaker Cells Array: the Transition from a Normal Activation to Atrial Fibrillation', Journal of Biological Cybernetics, February (1999);Vol. 80,No. 2, pp. 41-153.
[38] Sivan S. A. and Akselrod S., 'A single pacemaker cell model based on the phase response curve', Journal of Biological Cybernetics, July (1998);Vol. 79, No. 1, pp. 67-76.
[39] Hartley T.T., 'The Duffing Double Scroll', Proceedings of the American Control Conference, Pittsburgh, June (1989);pp. 419–423.

[40] Yoo B.and Ham W., 'Adaptive Fuzzy Sliding Mode Control of Nonlinear System', IEEE Trans. Fuzzy Syst., (1998); vol.6, pp.315- 321.
[41] Lee H., Kim E., Kang H.J.and Park M., 'A New Sliding-mode Control with Fuzzy Boundary Layer', Fuzzy Sets and Systems, May,(2001);vol. 120, no 1, pp. 135-143.
[42] Andrievskii B. R. and Fradkov A. L., 'Control of Chaos: Methods and Applications. I. Methods, Automation and Remote Control', May (2003);Vol. 64, No. 5, pp. 673-713.
[43] Wang J., Rad A.B., and Chan P.T., 'Indirect Adaptive Fuzzy Sliding Mode Control: Part I-Fuzzy Switching, Fuzzy Sets and Systems', August, (2001); vol. 122, no 1, pp. 21-30.
[44] Kim S.W.and Lee J.J., 'Design of a Fuzzy Controller with Fuzzy Sliding Surface, Fuzzy Sets and Systems', May, (1995);vol. 71, no 3, pp. 359-367.
[45] Boccaletti S., Grebogi C., Lai Y. C., 'Mancini H., and Maza D., The Control of Chaos: Theory and Applications', Physics Reports, (2000);Vol.329, pp. 103-197.
[46] Pecora L.and Caroll T., 'Synchronization in Chaotic Systems', Physics Review Letters, (1990);Vol. 64, No.8, pp. 821-824.
[47] Wang L.X., 'Stable adaptive fuzzy control of nonlinear systems', IEEE Trans. Fuzzy Syst., (1993); vol.1, pp.146-155.
[48] Abbas R., Aziz W.and Arif M., 'Prediction of Ventricular Tachyarrhythmia in Electrocardiogram Signal using Neuro-Wavelet Approach', National Conference on Emerging Technologies, (2004), pp. 82-87.
[49] Berstecher R.G., Palm R. and Unbehauen H.D., 'An adaptive fuzzy sliding-mode controller', IEEE Trans. Industrial Electron., vol. 48, (2001), pp. 18-31.
[50] Sivan S. A. and Akselrod S., 'A Pacemaker Cell Pair Model Based on the Phase Response Curve', Journal of Biological Cybernetics, July (1998); Vol. 79,No. 1, pp. 77-86.
[51] L.X. Wang, Stable adaptive fuzzy control of nonlinear systems, IEEE Trans. Fuzzy Syst., vol.1, (1993), pp.146-155.

Authors

Abdolhossein Ayoubi (1983), Jahrom, Iran. M.Sc. of Medical Informatics Technology in Biomedical Engineering Department, Amirkabir University of Technology, Tehran , Iran. Working as a specialist of Medical Informatics Technology, I have published 8 books in Createspace/Amazon Publication and one other book in Atraa publication, Iran, and several papers in Biomedical Engineering.

Moharram Kazemi (1972), Khoy, Iran. M.Sc. of Medical Informatics Technology, Amir Kabir Technical University, Biomedical department, Tehran, Iran. Working as a Cardiac Electrophysiology Clinical specialist, I published 2 books via Createspace/Amazon publication, and several papers in Biomedical engineering. Email Address: kazemi1az@yahoo.com, Tel: 0098121366802, Address: plaque:60 ,Third Floor ,39th Gisha St, Tehran , Iran. Postal Code 1447975547

Mohammad Sadegh Sanie (1977) Jahrom,Iran. MD in Anesthesia and Critical Care, a member of Scientific Board in Anesthesia and Critical Care in Jahrom University of Medical Sciences. I collaborate with two journals as their reviewer which include Anesthesia and Critical Care (AACC) and (Pars) Research Periodical, I have published 2 books in Createspace/Amazon Publication, and several papers in conferences. Sadegh_532@yahoo.com **,** Tel:00989177002599

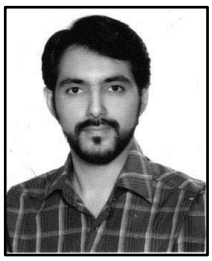

Saman Sobh Heydari (1976),Tabriz, Iran. M.Sc. of Medical Informatics Technology, Biomedical Engineering Department, Amirkabir University of Technology, Tehran , Iran; working as a specialist of Medical Informatics Technology, I published one book via Createspace/Amazon publication, and several papers in Biomedical Engineering. Email Address: saman303@yahoo.com; Tel : 00989166433448. Address: Plaque: 42, 2nd Baharan, Baharan Neighbor, Dezfoul, Khoozestan Province, Iran, Postal Code:6461687653